PROCEEDINGS, 49th Workshop on Geothermal Reservoir Engineering
Stanford University, Stanford, California, February 12-14, 2024
SGP-TR-227

Field Test of Thermoelectric Generators for Power Generation Using Low Temperature Industrial Waste Heat

Yuhao Zhu[1,2], Kewen Li[1,2,*], Mahlalela Bhekumuzi Mgijimi[1,2], Jifu He[1,2], Lei Wang[1,2], Aiwei Zheng[3], Xiaodong Wang[3], Hongyang Zhang[1,2] and Changwei Liu[1]

[1] China University of Geosciences (Beijing), 29 Xueyuan Road, Beijing 100083, China

[2] Key Laboratory of Marine Reservoir Evolution and Hydrocarbon Enrichment Mechanism, Ministry of Education, Beijing 100083, China

[3] Huayang New Material Technology Group Co., Ltd., Yangquan 045000, China

likewen@cugb.edu.cn

Keywords: Thermoelectric generators (TEG), Field test, Geothermal power generation, Waste heat recovery

ABSTRACT

Interest in thermoelectrics for waste heat recovery and geothermal energy has flourished in recent years, but China's installed geothermal power capacity has barely increased. Carbon neutralization brings new opportunities for geothermal energy development and utilization. This work investigates the innovation in geothermal power generation technology as an important part to accomplish the carbon neutralization goals. Thermoelectric generators (TEG) could be used for geothermal power generation and waste heat recovery, thus converting low-grade thermal energy into electricity. Since TEG works in a very simple manner as it converts thermal energy into electricity, it could fill part of the technical gaps in the development and utilization of low to medium temperature geothermal resources. For this work, we conducted the field tests of TEG using industrial waste heat from a gas power plant. The temperature was around 80 °C. The TEG units were hierarchically modular and easily expandable to fit any scale. The power output and efficiency of TEGs were influenced by temperature difference and fluid flow rate. At appropriate flow rates, a TEG unit with a volume of about 0.03 m^3 could generate a power of 150 W at a temperature difference of 60 °C. The power density and the power per unit area of the TEGs were investigated at various temperature differences, and were compared with those of diesel generators and photovoltaic (PV) panels, respectively. Additionally, in order to provide guidance and clue for TEG at commercial scales, we estimated the costs of TEG fabrication, installation and also the Levelized Cost of Electricity (LCOE) at various temperature differences. Many previous studies reported that TEG were mostly used for low-power microelectronic devices, but results from this study demonstrate the feasibility and the potential of TEG for large scale geothermal power generation and waste heat recovery.

1. INTRODUCTION

Crisis of fossil fuels has brought more interest in thermoelectrics for waste heat recovery and geothermal energy in recent years. China aims to achieve the peak of CO_2 emissions in 2030 and become carbon neutral before 2060 (known as “dual-carbon policy”) to tackle climate change. This goal is driving rapid growth in the development of renewable energy utilization while pushing heavily emitting industries to save energy and reduce emissions. Waste heat recovery (WHR) is commonly used in industrial applications. The launch of China Carbon Emission Trade Exchange (CCETE) brings huge economic benefits to companies in low-carbon industries. Companies seeking to become carbon neutral must reduce their own emissions rather than simply pay for emission reductions elsewhere.

Internal combustion engines have two important resources of heat exhaust that account for about 65-70% of the energy input: the exhaust system (about 35-40%) and the radiator (about 30%) (Burnete et al., 2022). WHR based on thermoelectric generators (TEG) could convert low-grade thermal energy directly into high-grade electric energy through a phenomenon called Seebeck effect, and this may be a solution to the problem of medium and low temperature power generation (Li et al., 2015). The potential of TEG for WHR has been theoretically studied and demonstrated in many laboratory scale works. However, there has been no practical and large-scale implementation of this technology in related industries. Many previous investigations on TEG applications for WHR were focused mainly on automotive exhaust and industrial applications. According to a summary (Ochieng et al., 2022), there are few studies with a power output of more than 100 W. Industrial WHR based on TEG requires more pilot tests at a larger scale.

Anderson and Brandon (2019) compared the performance of TEG with the Rankine cycle and found that the Rankine cycle is able to achieve superior thermal efficiencies at power outputs above 100 kW. In the range of 10 to 100 kW, the thermal efficiency of TEG is comparable to that of the Rankine cycle. Below 10 kW, the efficiency of the TEG is higher than that of the Rankine cycle.

Waste heat is available in various forms such as flue gas, exhaust gas from fossil fuel power plants, sewage and heated water, etc. Yadav et al. (2021) performed experiments to use TEG for harvesting waste heat from the billet casting industry. During the billet (average temperature at 540 °C) cooling process, 12 TEG units were placed between the absorber copper plate and water cooling block, and generated a total power output of 339 W. Børset et al. (2017) implemented a 0.25 m^2 TEG at a silicon plant for WHR from silicon during the casting process. The maximum power output reached 40.5 W at an average temperature difference of about 100 °C. Punin et al. (2019) investigated the heat transfer characteristics of a TEG system for low-grade WHR from a sugar industry. The average temperature of the

outer surface of the sugar boiler is usually about 200 °C. When the temperature difference between the hot and cold sides of TEG was 95°C, the maximum power output reached 126.15 W and the system efficiency reached 11.5%. Meng et al. (2017) proposed that the power out of TEG could reach about 1.47 kW/m^2 with a conversion efficiency of 4.5% for exhaust gas at 350 °C. At a lower temperature difference of 52 °C, the maximum output power and power density of the TEG reported by Van Toan et al. (2022) were 95.9 mW and 610.8 μW/cm^2, respectively.

Casi et al. (2021) built and tested a TEG at a rockwool manufacturing plant using fumes (340 °C) flowing in the pipe as the hot side and heat pipe heat exchangers as the cold side. During the test period, the average power output was 4.6 W with an efficiency of 2.38%. The optimization of the TEG at the rockwool manufacturing plant was carried out by Araiz et al. (2020) in terms of both power output and economic cost. The installation cost could be minimized to 10.6 €/W and the Levelized Cost of Electricity (LCOE) estimated for their design was about 0.15 €/kWh. After analyzing the power generation performance of TEGs of different sizes by numerical calculation methods, Miao et al. (2022) conducted a field test of TEG at a steel company with a maximum output of 80.5 W and a minimum power generation cost of 1.76 $/W. Their results demonstrated the potential of using TEG for WHR at a reasonable cost.

Small-scale TEG are often used to directly supply power to low-power electronic devices, rather than to the power grid. Huang et al. (2021) designed and tested a TEG for WHR from an atmospheric pressure plasma jet (APPJ) and powering a multi-functional monitoring system to monitor the temperature of APPJ and the surrounding air quality.

The design optimization of TEG lies mainly on the heat exchanger and advanced materials. Chen et al. (2022) designed a variable converging angle in each part of the heat exchanger so that the temperature difference applied to the thermoelectric modules was approximately the same in all parts. Their design increased the power output of TEG by 12.5%. Khalil et al. (2021) compared three cooling systems of a TEG installed on a chimney for WHR. TEGs with closed- and open-circuit liquid cooling systems could generate 8 and 45% more power output than those with heat pipes, respectively. Wang et al. (2020) proposed a WHR system with potassium heat pipes and skutterudite TEGs for passive thermal management and power generation. Cui et al. (2019) evaluated the power output of a porous annular TEG for WHR. This TEG consisted of p- and n-type porous thermoelectric foams (TEFs). The analysis showed that the porous structure could improve the performance of TEG compared to bulk TEG. Lee and Lee (2018) improved the compactness of TEG with printed circuit heat exchangers. The power density of the TEG reached 233.1 kW/m^3 at the inlet temperatures of 175°C (hot side) and 20°C (cold side). At a temperature difference of 250 °C, Maksymuk et al. (2022) used the Spark Plasma Sintering technique to increase the efficiency of a thermoelectric unicouple from 3-6% to ~8%.

Li et al. (2021) conducted geothermal field tests with a 6-layer TEG apparatus which generated about 500 W electricity at a temperature of 176 °C. They demonstrated that the cost of TEGs is less than that of solar PV panels if capacity factor is considered. However, it is still a big question and a great challenge whether it is possible to use TEG devices to generate power at a relatively large scale from waste heat resources with a temperature of less than 100 °C. The waste heat resources within such a temperature range are huge around the world. As reported by Li et al. (2021, 2020), the expandability of a TEG apparatus is important to generate power at a large scale but the maximum number of layers in their TEG systems was only 6.

In this work, we manufactured two TEG devices, one with 10 layers and the other with 20 layers, and conducted field tests using the waste heat with a temperature of 80 °C at a gas power plant located in Shanxi province, China. The power output and the efficiency of the TEG devices were measured on-site at various temperatures and flow rates. The field test data were analyzed and discussed. The costs of the TEG devices were estimated at different temperatures.

2. FIELD TESTS

The gas power plant is located at a coal mining area with abundant coal-bed methane resources. The gas power plant has three gas generators of 1.8 MW with a total installed capacity of 5.4 MW. The waste heat mainly exists in the exhaust gas emissions and the engine cooling closed-loop. During winter season (about four months per year), the waste heat is transferred into the heating network through heat exchangers for indoor heating. During summer season, the waste heat is discharged into the air by fans. The overview of the WHR system with TEG at the gas power plant is shown in Fig. 1. The schematic and the arrangement of the TEG devices with the piping network from the gas generators at the gas power plant is schematically shown in Fig. 2.

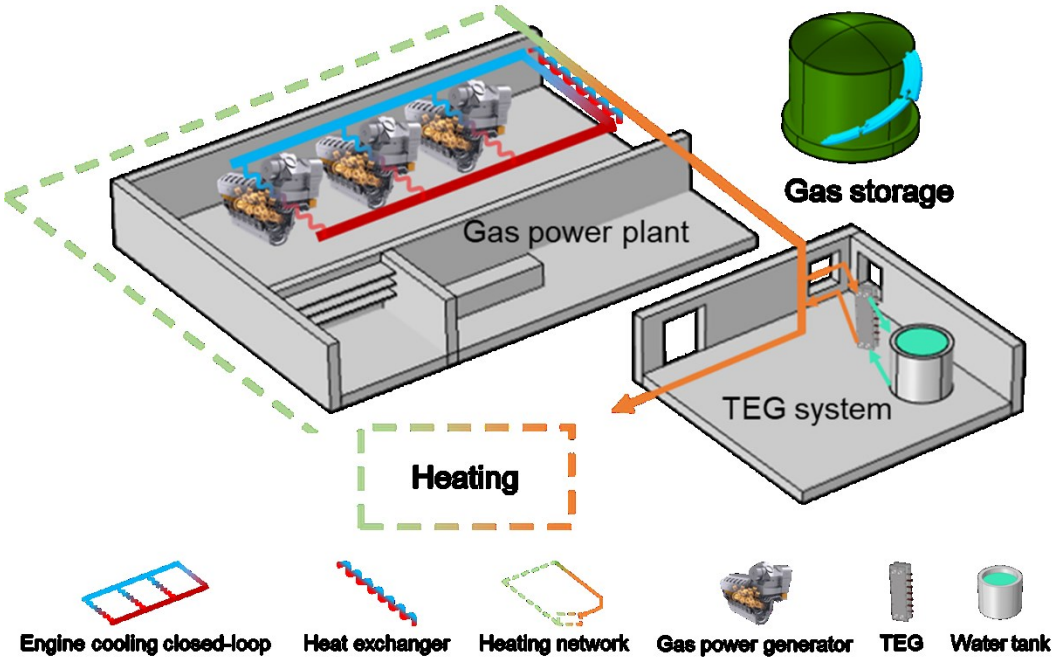

Figure 1: The overview of the WHR system at a gas power plant.

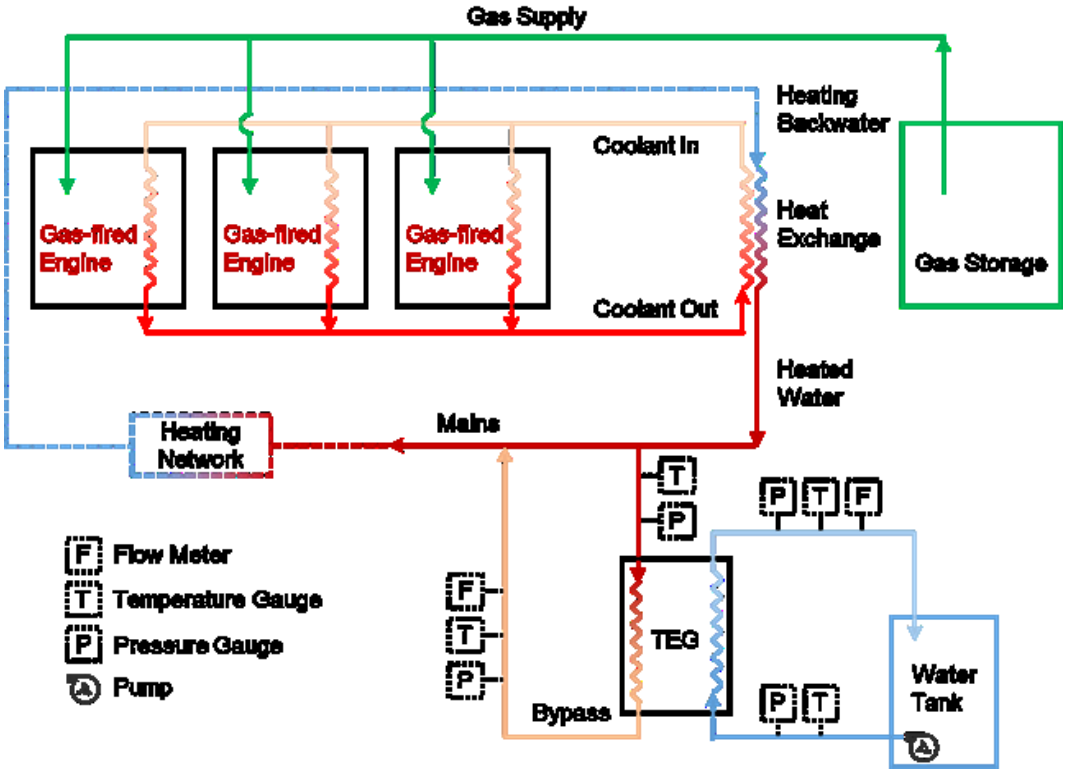

Figure 2: The schematic and the arrangement of the TEG with the piping network from the gas generators at the gas power plant.

In order to maintain the operating temperature of engines, the inlet temperature of coolant (ethylene glycol) must be kept between 76 - 78 °C and the outlet temperature below 90 °C. A large amount of waste heat was carried out by the coolant flowing in a closed-loop. Especially in summer, the outlet temperature of coolant could reach between 92 - 93 °C, close to the shutdown temperature of 95 °C. The

coolant of engines was cooled by an external heat exchanger and then flowed back to the gas generators. The heat in the engine cooling closed-loop was transferred to the heating network through the external exchanger for external use. The working fluid in the heating network was water. The TEG was installed in a bypass channel parallel to the mains of heating network, as shown in Fig. 2.

2.1 Installation of TEG

To solve the scalability problem of existing TEG units, we designed a lab-scale TEG unit (Li et al., 2020) with a hierarchical structure that can be easily scaled up, as shown in Fig. 3. In this field test, the TEG was expanded to 10 and 20 layers, respectively. The external heat exchanger between the engine cooling closed-loop and the heating network was well suited for installing TEG. Considering the safety issues and in order not to interfere with the operation of gas generators, we didn't choose to install the TEG to replace the external heat exchanger. The installation site of TEG was chosen in an area where the heating network passed through and near a water tank.

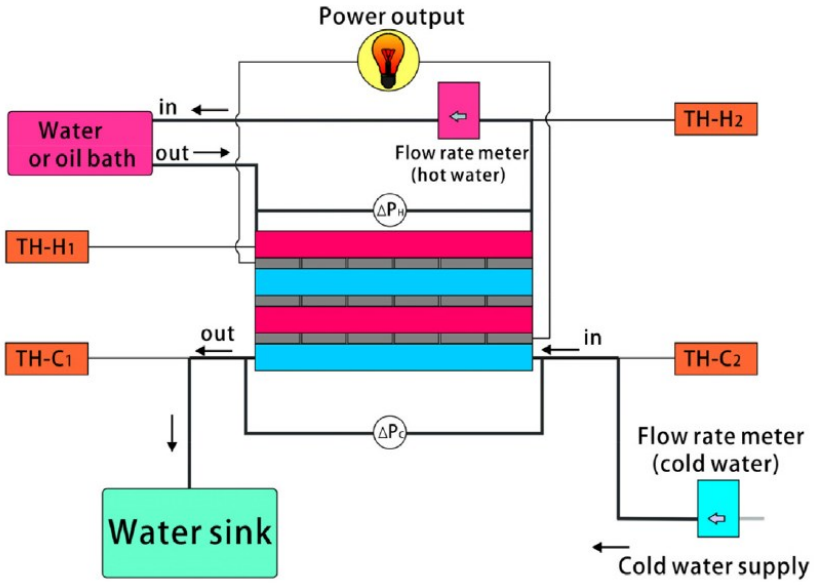

(a) The schematic of the labscale thermoelectric power generation system (Li et al., 2020).

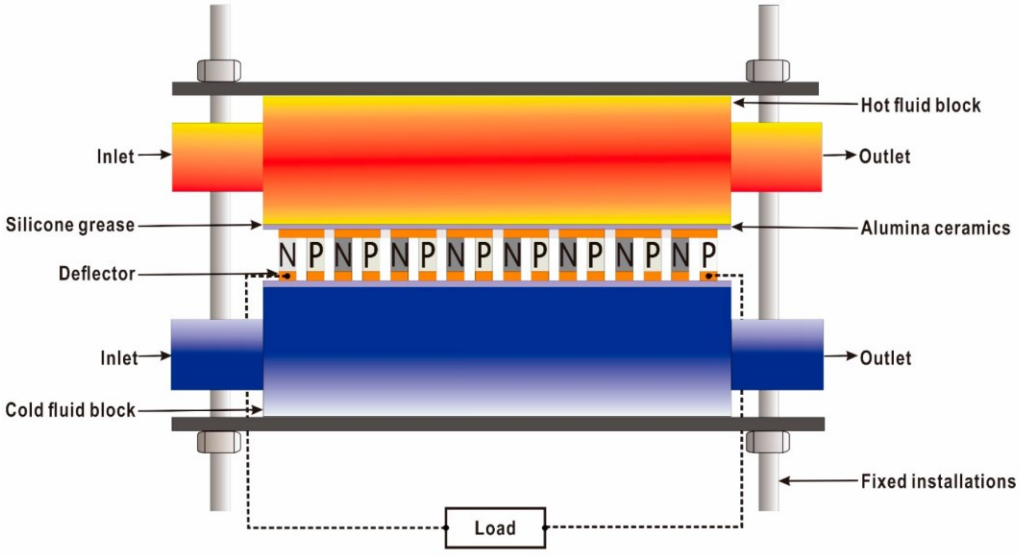

(b) The schematic of single thermoelectric module test (Chen et al., 2017).

Figure 3: The schematic diagram. (a) The lab-scale TEG unit with a hierarchical structure. (b) The single thermoelectric module.

As shown in Fig. 4, one of the TEG devices (20 layers) was installed nearby the windows. The hot flow channel of TEG was connected to the pipelines via two heat insulated tubes. The valves allowed to control the pressure and flow rate of hot water in the tubes. The cold flow channel was connected to a water tank. Another TEG (10 layers) was connected in the same way in the field tests. The 10-layer TEG contains 24 modules per layer and the 20-layer TEG contains 18 thermoelectric modules per layer.

Figure 4: One of the TEG devices (20 layers) installed for field tests.

2.2 Test Setup

Fig. 5 shows the photos of TEG devices ready for field tests. The TEG devices were wrapped with insulating tape for safety during the tests. The size of the 20-layer TEG was about 0.3 m × 0.2 m × 0.55 m, and the size of the 10-layer TEG was about 0.18 m × 0.2 m × 0.7 m. The schematic of the test setup of the TEG is shown in Fig. 6. The selected part of the pipelines was fitted with pressure gauges, temperature gauges, control valves, and multiple outlets. Two flow meters (FLOWSTAR, Yancheng, China) were installed at the outlets of the hot and cold sides respectively. An electronic load (IT8211, ITECH, Nanjing, China) was used to provide external load and measure the voltage, current, and power output. Depending on the thermoelectric modules contained in each TEG device, the electronic load was set to the appropriate values corresponding to the internal resistance of each TEG to obtain the maximum power output.

The inlet and outlet of the hot flow channel were connected to the heating network with rubber hoses. The inlet and outlet of the cold flow channel were connected to the water tank with rubber hoses and circulated by a pump. The temperature of hot water was between 70 and 90 °C. The temperature of cold water was around 20 °C.

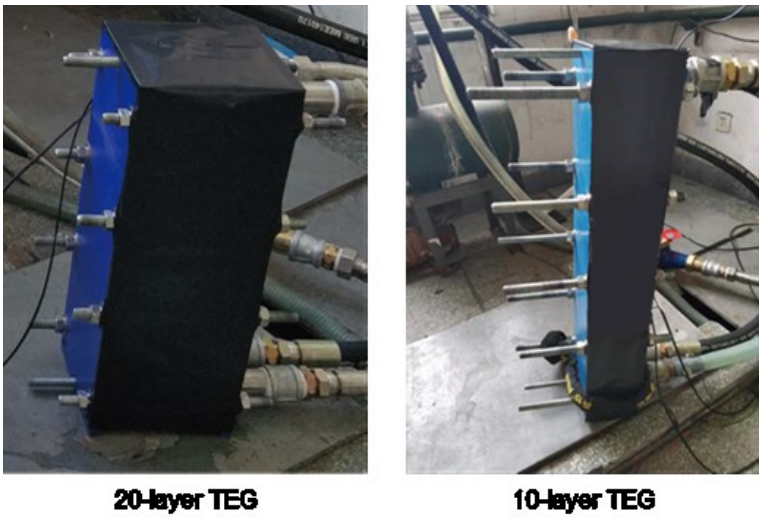

Figure 5: Photos of the TEG ready for the field tests.

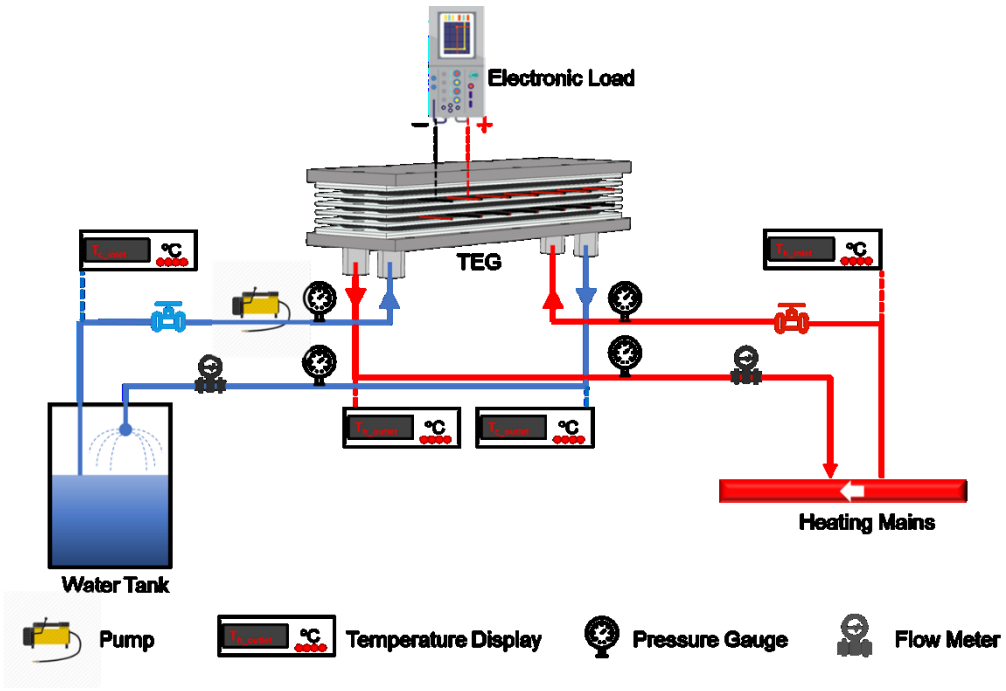

Figure 6: The schematic representation of the experimental setup of the TEG devices.

3. RESULTS AND DISCUSSIONS

3.1 Effect of Temperature Difference on Power Output

Temperature difference is one of the most important factors influencing the performance of TEG. In the laboratory experiments reported by Li et al. (2020), the power output of TEG was directly proportional to the temperature difference. In field tests, it is usually not convenient to adjust the water temperature at winter. Because of this reason, the results measured at various temperature differences in this study were relatively few and did not vary much from each other. The temperature of the hot fluid in this field test was between 70 – 80 °C, and the temperature of the cooling water was about 20 °C. We quoted the data from previous geothermal field test (2021) at a temperature of 176 °C for comparison. The coolant in the geothermal field test was water at a temperature of 24 °C. The TEG apparatus used in the geothermal field test had 6 layers, one of which did not work properly. To test the expandability of TEG, the TEG devices in this field test contained more layers, 10 and 20 layers, respectively. So the average power output per layer was used instead of the total power output to investigate the power output at different temperatures.

Fig. 7 shows the comparison of the average power output per layer of TEG in the field tests and laboratory experiments, including the data from this study and those reported by Li et al. (2021, 2020). The power output per layer in this field test is almost the same as the power output per layer in the laboratory experiment. The power output increased with the temperature difference. The test results at low temperatures correlate well with the results of high temperature field tests.

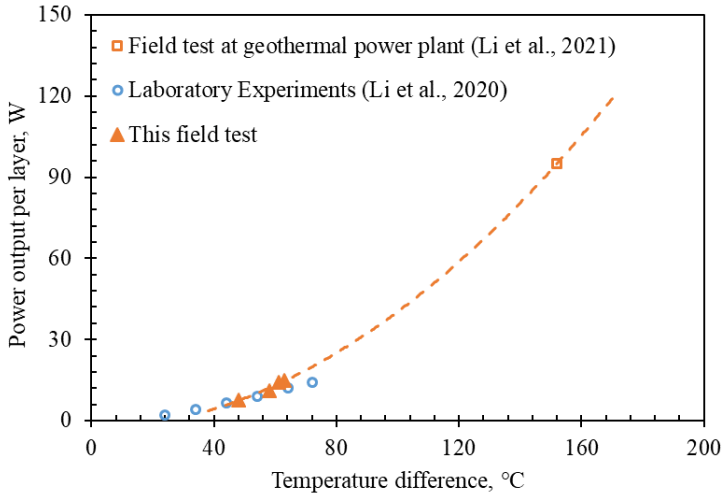

Figure 7: The power output per layer vs. temperature differences.

3.2 Effect of Flow Rate on Power Output

We measured the voltage, current, and power output of the TEG devices at different flow rates on both hot and cold fluids. Although the flow rate on the hot side was adjustable, the range was limited to 0-7 m^3/h. The flow rate on the cold side was adjustable from 0 to 5 m^3/h. During the tests, the flow rate varied only on one side and was constant at 3 m^3/h on the other side, and the temperature difference was around 60 °C (± 1 °C).

The power output of the TEG device at different hot and cold flow rates are plotted in Figs. 8 and 9, respectively. The power output increased with the flow rates on both hot and cold sides, and the growth rate decreased gradually. The 20-layer TEG device had higher total power output than the 10-layer TEG, in particular at greater flow rates. Two times the power output of 10-layer TEG matches extremely well with the power of 20-layer TEG. After the flow rate increased to some extent, expanding the number of layers of TEG could be more efficient to enhance the power output than continuing to increase the flow rate. The TEG devices designed and manufactured in this study were hierarchically modular and easily expandable, which is suitable for coping with complex industrial heat resources.

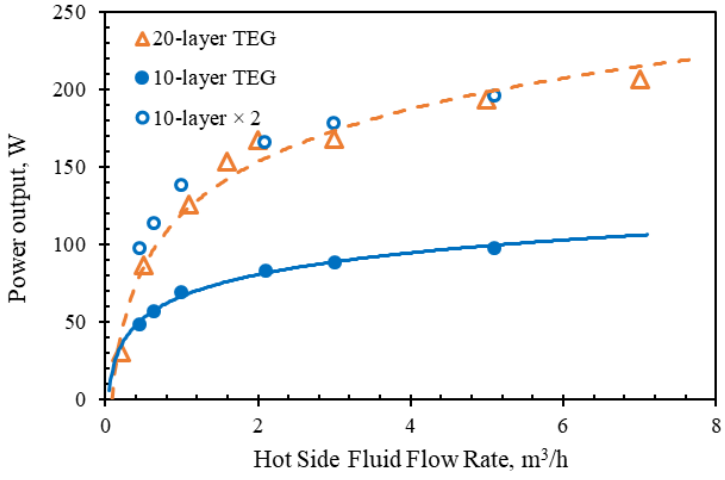

Figure 8: The total power output of the TEG devices at different flow rates on the hot side (water flow rate on the cold side was 3 m^3/h and the temperature difference was 60 °C (± 1 °C)).

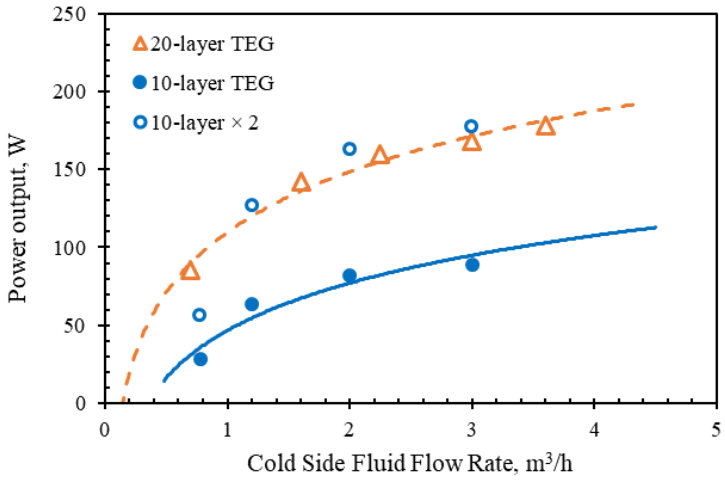

Figure 9: The total power output of the TEG devices at different flow rates on the cold side (water flow rate on the hot side was 3 m^3/h and the temperature difference was 60 °C (± 1 °C)).

3.3 Effect of Temperature Difference on Efficiency

The efficiency of TEG η is defined by W_{TEG}/Q_h, where W_{TEG} is the power output of TEG (W), and Q_h is the heat flux on the hot side (W). Fig. 10 shows the efficiency of the TEG devices at different temperature differences. In these field tests, the efficiency of TEG was similar to the laboratory results measured and reported by Li et al (2020). Overall, the efficiency increased with temperature difference. The highest efficiency of the TEG devices in this field test was about 1.72% at a temperature difference of 60 °C. In contrast, the efficiency of TEG in the geothermal field test (Li et al., 2021) rose to more than 5% at a temperature difference of 152 °C (the exact value was related to the flow rate). Niu et al. (2009) conducted an experimental study at lower flow rates (0.4 m^3/h) and the maximum conversion efficiency increased to 4.44% at a temperature difference of 120 °C. The efficiency at the same temperature difference varies somewhat in different studies due to differences in fluid flow rates and the design of TEGs.

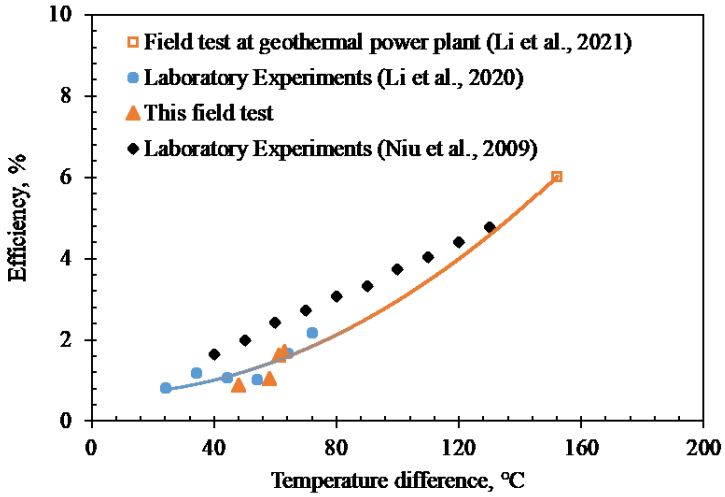

Figure 10: The efficiency of the TEG devices at different temperature differences.

3.4 Effect of Flow Rate on Efficiency

Fig. 11 shows the efficiency of TEG at different flow rates on the hot side when the water flow rate on the cold side was 3 m^3/h and the temperature difference was 60 °C (± 1 °C). The overall trend in efficiency decreased gradually with the increase in hot flow rate. For a heat resource at a specific temperature, a greater flow rate means more heat input to the TEG. If the increase in power couldn't match the increase in hot flow rate, the efficiency will decrease. It is worth to note that there is a peak phase of efficiency at hot flow rates between 2 and 3 m^3/h. As can be seen in Fig. 8, the power output had also increased to a higher range at hot flow rates between 2 and 3 m^3/h. The

hot flow rate range of 2-3 m^3/h might be a reasonable range to achieve high power output and high efficiency of the TEGs at the same time in these cases. The efficiency of TEGs gradually decreased after the hot flow rate exceeded 3 m^3/h, and the efficiency of the 20-layer TEG was higher than that of the 10-layer TEG.

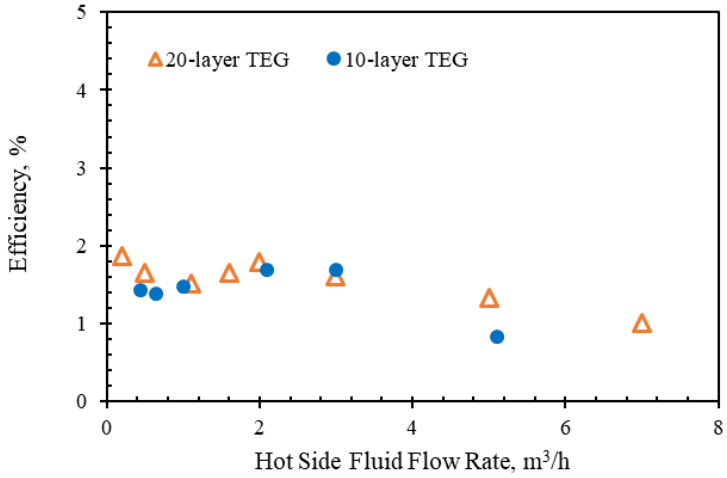

Figure 11: The efficiency of the TEG devices at different flow rates on the hot side (water flow rate on the cold side was 3 m^3/h and the temperature difference was 60 °C (± 1 °C)).

The efficiency of the TEG devices at different flow rates on the cold side is plotted in Fig. 12 when the water flow rate on the hot side was 3 m^3/h and the temperature difference was 60 °C (± 1 °C). The efficiency of the 20-layer TEG increased with the cold flow rate until the cold flow rate reached 2 m^3/h. The efficiency of the 10-layer TEG also increased with the cold flow rate and slightly exceeded the efficiency of 20-layer TEG at a cold flow rate of 3 m^3/h. When the thermal energy was fed into the TEG at a constant rate, a greater cold flow rate could help the TEG absorb more thermal energy and convert it into electricity, while also obtaining a higher efficiency. The TEG could have a maximum efficiency at a cold flow range from 2 to 3 m^3/h in these cases.

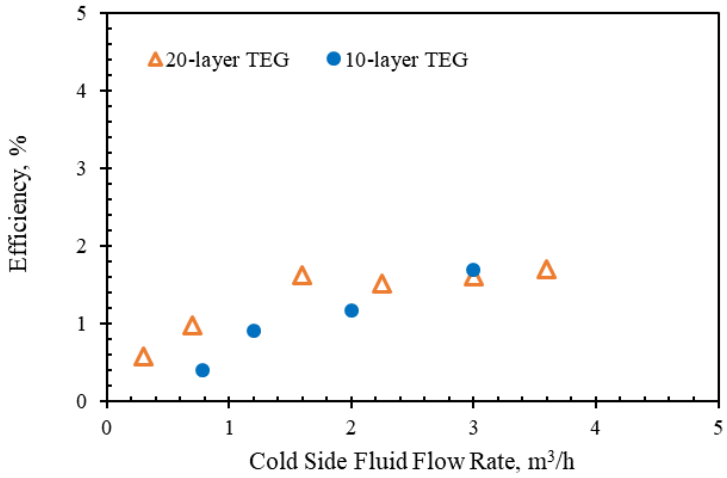

Figure 12: The efficiency of the TEG devices at different flow rates on the cold side (water flow rate on the hot side was 3 m^3/h and the temperature difference was 60 °C (± 1 °C)).

The efficiency of 10-layer and 20-layer TEG are almost the same on varying hot fluid flow rates. When changing the cold fluid flow rate, the efficiency of the 10-layer TEG is similar to that of the 20-layer TEG. As discussed above, the proposed 10-layer and 20-layer TEG devices could yield high power output and high efficiency at the same time when the flow rates on both the hot and cold sides were simultaneously in the range of 2-3 m^3/h.

3.5 Power Density and Power per Unit Area

Fig. 13 shows that the power density of TEG at various temperature differences. Most of the applications of TEG are small in size, even less than 1 W. Although some small TEGs have high power density, they have low potential for large-scale applications or are still in the conceptual design stage. At temperature differences above 106 °C, the power density of the TEG in this study could reach the level of diesel generators (10kW/m^3 or greater). As the temperature difference increases, the power density of TEG increases further. The power density of TEG could reach 16 kW/m^3 at a temperature difference of 150 °C, which is at the same level as XD5000E Model #6864 (one of the most popular diesel generators on the market).

Figure 14 shows the power per unit area of TEG at different temperature differences. The power per unit area of PV panels is in the range of 150 – 250 W/m^2. The power per unit area of TEG could reach 150 W/m^2 at temperature difference as low as 60 °C. The power per unit area of TEG will exceed that of PV panels at temperature differences above 80°C. Lee and Lee (2018) reported a TEG with a very high power density of 233.1 kW/m^2 at a temperature difference of 155 °C, which would be more advantageous if their design could be scaled up. The hierarchically expandable TEG in this study makes it possible to scale up while maintaining high power density.

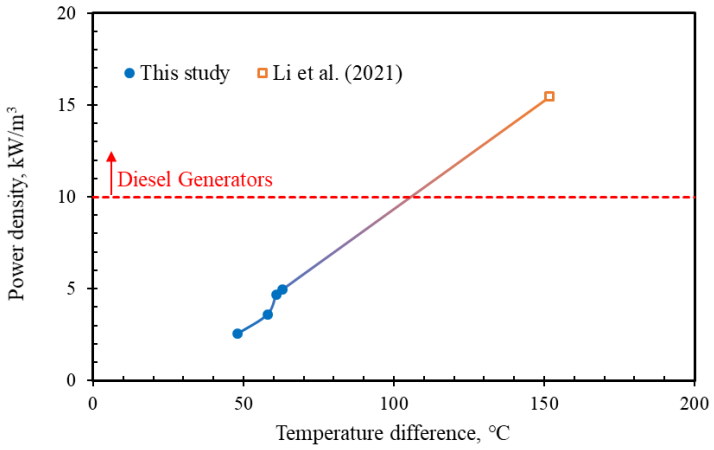

Figure 13: The power density of the TEG devices at different temperature difference.

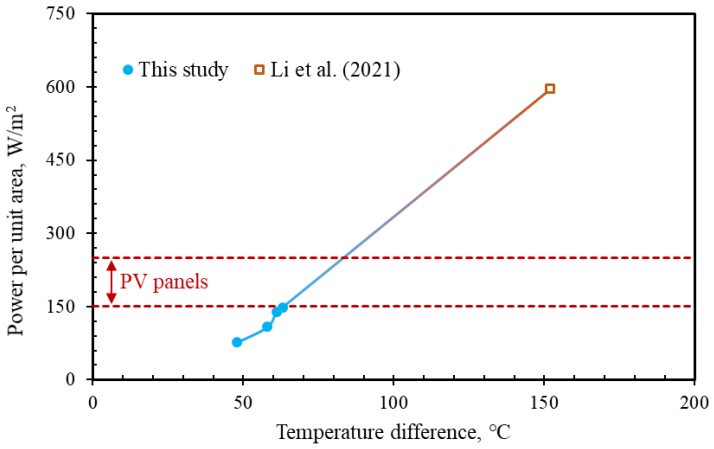

Figure 14: The power per unit area of the TEG devices at different temperature difference.

3.6 Cost Estimation

Based on the results of the field tests conducted in this study and the geothermal field tests by Li et al. (2021), the installation cost ($/kW) and the Levelized Cost of Electricity (LCOE) of TEG at different temperature differences were calculated with reference to the cost data of geothermal power generation (from International Renewable Energy Agency). For the same installation cost, the LCOE of thermoelectric power generation is seen as similar to that of geothermal power generation. The estimated cost data are shown in Fig. 15. The LCOE of TEG could be comparable with the average cost of fossil fuels when the temperature difference reaches 150 °C, which

means that thermoelectric power generation could be conducted at a reasonable cost. As reported by Li et al. (2021), the cost of TEG is also attractive compared with PV panels if the capacity factor were considered.

Fig. 16 shows the capacity factor of different technology in 2020. The capacity factor of TEG is similar to that of geothermal, which could reach more than 80%. The capacity factor of PV is about 20%, which is only one quarter of that of TEG. The TEGs are more advantageous when connected to the grid because the instability of PV and wind power can cause severe oscillations to the grid.

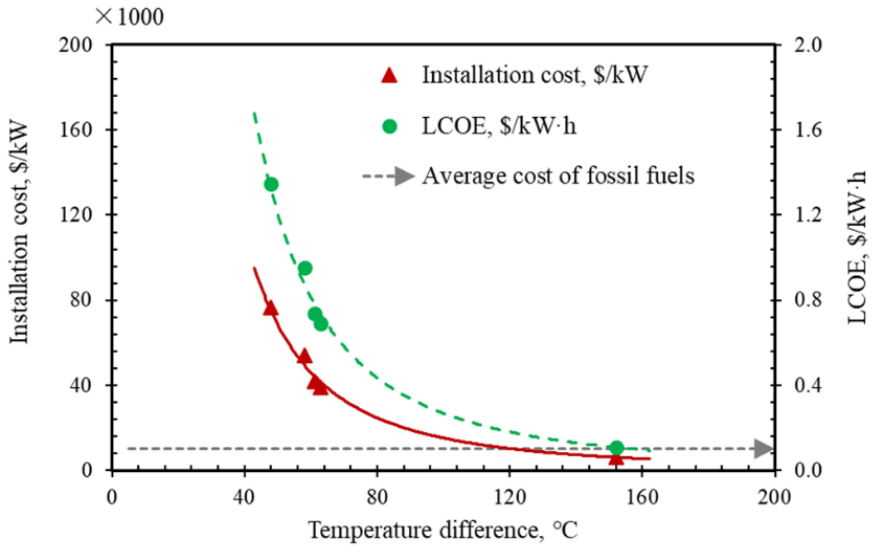

Figure 15: The installation cost and LCOE of TEG at different temperature differences.

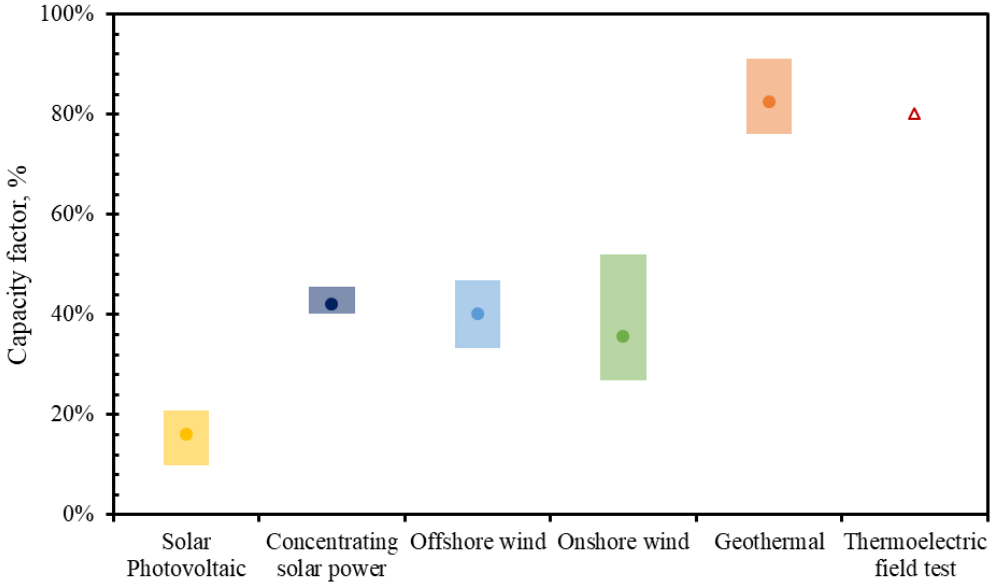

Figure 16: Global weighted-average utility-scale capacity factor by technology, 2020.

Fig. 17 shows the installation cost of TEG at different temperature difference compared to other renewable energy sources in different years. With the development of technology, the installation costs of power generation from various renewable energy sources have shown a decreasing trend along with some fluctuations. The installation cost of TEG decreases with increasing temperature difference. At a temperature difference of 150 ° C, the installation cost of TEG is in the middle of the installation cost of renewable energy.

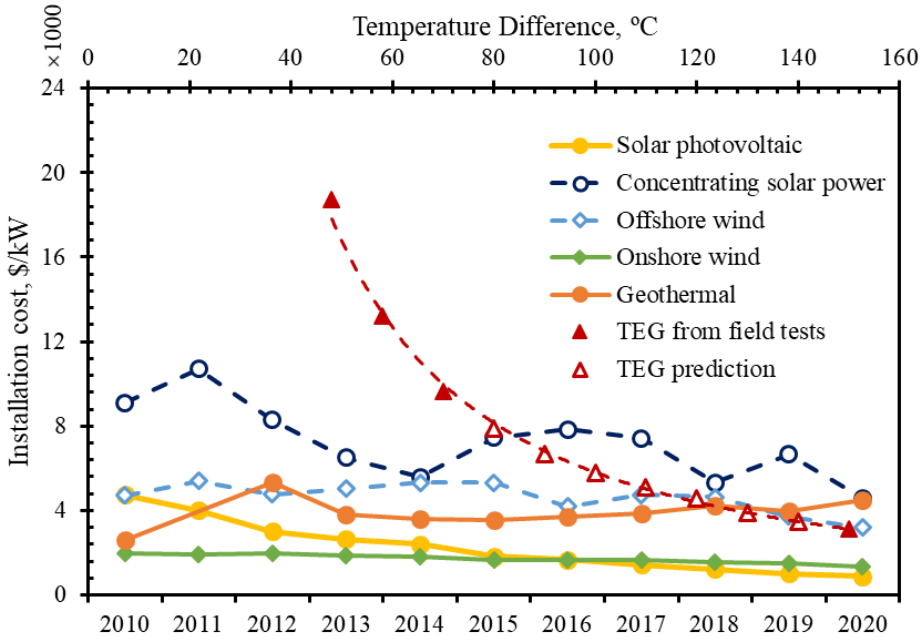

Figure 17: The installation cost of TEG at different temperature difference compared to other renewable energy sources in different years.

CONCLUSIONS

According to the field test results, the following conclusions may be drawn:

(1) We have designed and manufactured two TEG devices with 10 and 20 layers (the highest number of layers reported) respectively and conducted power generation tests at temperatures as lower as 80 °C. The number of the layers in this type of TEG device is expandable, which provides a possible solution to scaling up TEG power generation to a commercial size.

(2) At a temperature difference of 60 °C and a flow rate of 3 m^3/h on both hot and cold sides, the 10- and the 20-layer TEG devices could generate about 88.8 and 167.8 W respectively. The power output generated by the two devices is almost directly proportional to the number of layers. This feature is important because it may be very helpful to deliver the electricity to the load in terms of stability, practicability, and low cost while commercializing TEG technology.

(3) The efficiency of the 10-layer TEG devices is almost the same as that of the 20-layer TEG device, which may increase, stay constant, or even decrease with the increase in the flow rates on the hot and cold sides. Most importantly, the efficiency of the 10-layer and the 20-layer TEG devices measured at low temperatures exhibit similar trend with those measured in the laboratory and in the field tests conducted at high temperatures. This implies that the efficiency of the TEG devices measured at different situations is almost the same at the same temperature difference, regardless of the number of layers, in the laboratory and at the geothermal wells.

(4) The TEG devices could yield relatively high power output and high efficiency at the same time in an optimal flow rate range of 2-3 m^3/h on both the hot and cold sides. The optimal flow rate may change with the range of temperature and other conditions.

(5) The cost of the TEG devices decreases with the increase in the temperature difference between the hot and cold sides. It may be lower than that of solar PV panels if availability and capacity factor are considered.

(6) The power density and power per unit area of TEG both increase with the temperature difference. The hierarchically expandable design allows the TEG devices to achieve power densities comparable to diesel generators and to exceed the power per unit area of PV panels.

ACKNOWLEDGEMENT

This work was financially supported by Huayang New Material Technology Group Co., Ltd. Their contributions are gratefully acknowledged.

REFERENCES

Anderson, K., & Brandon, N. (2019). Techno-economic analysis of thermoelectrics for waste heat recovery. Energy Sources, Part B: Economics, Planning, and Policy, 14(4), 147-157.

Araiz, M., Casi, Á., Catalán, L., Martínez, Á., & Astrain, D. (2020). Prospects of waste-heat recovery from a real industry using thermoelectric generators: Economic and power output analysis. Energy Conversion and Management, 205, 112376.

Børset, M. T., Wilhelmsen, Ø., Kjelstrup, S., & Burheim, O. S. (2017). Exploring the potential for waste heat recovery during metal casting with thermoelectric generators: On-site experiments and mathematical modeling. *Energy*, *118*, 865-875.

Burnete, N. V., Mariasiu, F., Depcik, C., Barabas, I., & Moldovanu, D. (2022). Review of thermoelectric generation for internal combustion engine waste heat recovery. *Progress in Energy and Combustion Science*, *91*, 101009.

Casi, Á., Araiz, M., Catalán, L., & Astrain, D. (2021). Thermoelectric heat recovery in a real industry: From laboratory optimization to reality. *Applied Thermal Engineering*, *184*, 116275.

Chen, J., Li, K., Liu, C., Li, M., Lv, Y., Jia, L., & Jiang, S. (2017). Enhanced efficiency of thermoelectric generator by optimizing mechanical and electrical structures. *Energies*, *10*(9), 1329.

Chen, J., Wang, R., Luo, D., & Zhou, W. (2022). Performance optimization of a segmented converging thermoelectric generator for waste heat recovery. *Applied Thermal Engineering*, *202*, 117843.

Cui, Y. J., Wang, B. L., Wang, K. F., & Zheng, L. (2019). Power output evaluation of a porous annular thermoelectric generator for waste heat harvesting. *International Journal of Heat and Mass Transfer*, *137*, 979-989.

Huang, M. J., Lin, Y. H., Hsu, P. C., & Juang, J. Y. (2021). A TEG-based waste heat recovery system for atmospheric pressure plasma jets: Model prediction and experimental verification. *Applied Thermal Engineering*, *189*, 116693.

Khalil, H., Saito, T., & Hassan, H. (2022). Comparative study of heat pipes and liquid-cooling systems with thermoelectric generators for heat recovery from chimneys. *International Journal of Energy Research*, *46*(3), 2546-2557.

Lee, W., & Lee, J. (2018). Development of a compact thermoelectric generator consisting of printed circuit heat exchangers. *Energy Conversion and Management*, *171*, 1302-1310.

Li, K., Bian, H., Liu, C., Zhang, D., & Yang, Y. (2015). Comparison of geothermal with solar and wind power generation systems. *Renewable and Sustainable Energy Reviews*, *42*, 1464-1474.

Li, K., Garrison, G., Moore, M., Zhu, Y., Liu, C., Horne, R., & Petty, S. (2020). An expandable thermoelectric power generator and the experimental studies on power output. *International Journal of Heat and Mass Transfer*, *160*, 120205.

Li, K., Garrison, G., Zhu, Y., Horne, R., & Petty, S. (2021a). Cost estimation of thermoelectric generators. In *Proceedings of the 46th Workshop on Geothermal Reservoir Engineering, Stanford, CA, USA* (pp. 16-18).

Li, K., Garrison, G., Zhu, Y., Moore, M., Liu, C., Hepper, J., ... & Petty, S. (2021b). Thermoelectric power generator: Field test at Bottle Rock geothermal power plant. *Journal of Power Sources*, *485*, 229266.

Maksymuk, M., Dzundza, B., Matkivsky, O., Horichok, I., Shneck, R., & Dashevsky, Z. (2022). Development of the high performance thermoelectric unicouple based on Bi2Te3 compounds. *Journal of Power Sources*, *530*, 231301.

Meng F, Chen L, Feng Y, et al. Thermoelectric generator for industrial gas phase waste heat recovery[J]. Energy, 2017, 135: 83-90.

Miao, Z., Meng, X., & Liu, L. (2022). Analyzing and optimizing the power generation performance of thermoelectric generators based on an industrial environment. *Journal of Power Sources*, *541*, 231699.

Niu, X., Yu, J., & Wang, S. (2009). Experimental study on low-temperature waste heat thermoelectric generator. *Journal of Power Sources*, *188*(2), 621-626.

Ochieng, A. O., Megahed, T. F., Ookawara, S., & Hassan, H. (2022). Comprehensive review in waste heat recovery in different thermal energy-consuming processes using thermoelectric generators for electrical power generation. *Process Safety and Environmental Protection*, *162*, 134-154.

Punin, W., Maneewan, S., & Punlek, C. (2019). Heat transfer characteristics of a thermoelectric power generator system for low-grade waste heat recovery from the sugar industry. *Heat and Mass Transfer*, *55*, 979-991.

Van Toan, N., Tuoi, T. T. K., & Ono, T. (2022). High-performance flexible thermoelectric generator for self-powered wireless BLE sensing systems. *Journal of Power Sources*, *536*, 231504.

Wang, C., Tang, S., Liu, X., Su, G. H., Tian, W., & Qiu, S. (2020). Experimental study on heat pipe thermoelectric generator for industrial high temperature waste heat recovery. *Applied Thermal Engineering*, *175*, 115299.

Yadav, S., Liu, J., Kong, M. S., Yoon, Y. G., & Kim, S. C. (2021). Heat Transfer Characteristics of Thermoelectric Generator System for Waste Heat Recovery from a Billet Casting Process: Experimental and Numerical Analysis. *Energies*, *14*(3), 601.